Antilock Brake System With a Continuous Wheel Slip Control to Maximize the Braking Performance and the Ride Quality

Seibum B. Choi

***Abstract*—In this paper, a new type of antilock brake system (ABS) algorithm is developed. A full-time feedback control algorithm differentiates the new ABS from rule-based conventional ABS algorithms. The rear wheels are controlled to create limit cycles around the peak friction slip points. From the cycling patterns of the rear wheels, the optimal slips are defined. The front wheels are controlled to track the optimal slips defined by monitoring the behaviors of the rear wheels. The new algorithm can be implemented on any production ABS hardware without any modification or extra sensors. The test results show significant performance improvement in both the stopping distance and the noise, vibration, and harshness on homogeneous surfaces, and also quick detection of surface transition. The robustness of the new ABS algorithm is proven by vehicle tests on various speeds, surfaces, and driving conditions.**

***Index Terms*—Antilock braking system (ABS), brake system, continuous slip, feedback control, limit cycle.**

NOMENCLATURE

a_c :	introduced brake control lag
DD:	double differential
F_z :	tire normal force
FWD:	front-wheel drive
I_w :	wheel angular moment of inertia
k_0 :	slope of locally linearized μ-slip curves
k_p :	control proportional gain
k_d :	control derivative gain
PD:	proportional and differential
P_B :	wheel brake pressure
R:	tire nominal radius
RWD:	rear-wheel drive
S:	Laplace Transform
T_B :	wheel brake torque
V_{car} :	absolute vehicle speed equivalent to the free rotating wheel speed
V_w :	wheel speed
λ :	wheel slip
λ_{Rdes} :	desired slip of rear wheels equivalent to ω_{Rdes}
μ :	tire-to-surface friction coefficient
ω :	wheel angular velocity
ω_{Fdes} :	desired front-wheel angular velocity
ω_{Rdes} :	desired rear-wheel angular velocity
4WD:	four-wheel drive

Manuscript received November 5, 2006; revised July 2, 2007. Manuscript received in final form October 3, 2007. First published March 31, 2008; last published July 30, 2008 (projected). Recommended by Associate Editor R. Rajamani.

The author is with the Graduate School of Automobile Technology, Korea Advanced Institute of Science and Technology, Daejeon, 305-701, Korea (e-mail: sbchoi@kaist.ac.kr).

Digital Object Identifier 10.1109/TCST.2007.916308

I. INTRODUCTION

VEHICLE antilock brake systems (ABS) have been used and evolved for about three decades since they came into widespread use in production cars in 1978 developed by Bosch [1]. ABS was designed to keep a vehicle steerable and stable during heavy braking moments by preventing wheel lock. There have been no major changes to the original rule-based control architecture. However, there have been many minor rules added on to the existing control algorithm to refine the performance. As a result, the rule-based control algorithm has ended up with hundreds of trimming parameters. Wheel velocities are controlled through the modes of pressure dump, apply, and hold. At each mode, hydraulic valves on each wheel are commanded to open or to close based upon very complex rules. Due to the complexity of the rules, tuning of the control parameters is very time consuming. Also, the switching between control modes causes the wheel velocity to cycle around a peak tire-to-road friction slip point. A certain level of the cycling is inevitable to find the optimal slip point especially when individual wheel brake pressure is not measured. However, the excessive amount of cycling deteriorates braking performance as well as ride quality and vehicle-handling stability. Especially, cycling of front wheels on high-friction (μ) surfaces makes the ride very harsh.

There have been other efforts to enhance braking performance as well as ride quality by applying modern state feedback control methods. The results look promising. However, most of the methods need the information of full vehicle states, e.g., absolute vehicle speed, wheel brake pressure, the peak of surface-to-tire friction-slip curves, and surface type as well as extremely fast brake actuators [2]–[12]. These vehicle states, surface condition information, and fast actuators are available at an extra cost, but it is hard to justify the hefty extra cost for the benefits. ABS controls using other advanced types of brake actuators suffer the similar cost-versus-benefit issues [13]–[18].

In this paper, a new continuous wheel slip ABS algorithm is developed. In the new ABS algorithm, rule-based control of wheel velocity is reduced to the very minimum. Rear wheels cycle independently through pressure apply, hold, and dump modes, but the cycling is done by continuous feedback control. While cycling rear wheel speeds, the wheel peak slips that maximize tire-to-road friction are estimated. From the estimated peak slips, reference velocities of front wheels are calculated. The front wheels are controlled continuously to track the reference velocities. By the continuous tracking control of front wheels without cycling, braking performance is maximized and

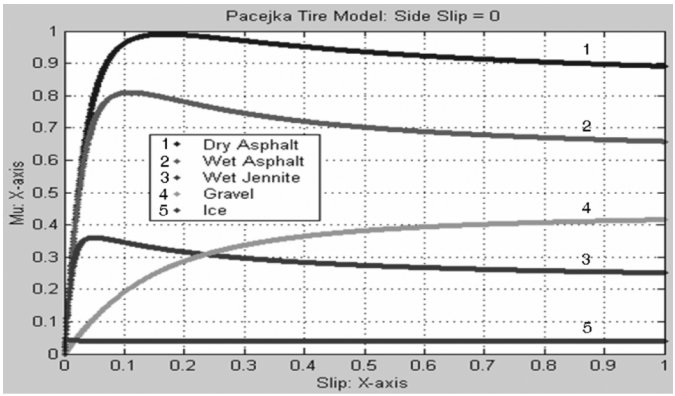

Fig. 1. Typical tire longitudinal friction μ-slip curves.

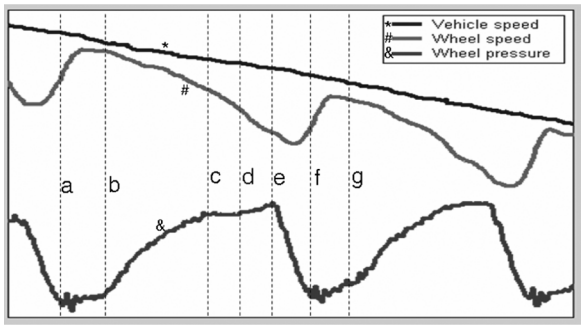

Fig. 2. Typical data trace of a conventional ABS on a homogeneous surface.

ride quality is improved significantly. The new ABS algorithm is implemented on a conventional production ABS harness using production sensors and brake actuators.

II. Tire

Tires are the hard-working key element of ABS controls. There have been many efforts to model tires mathematically. Generally speaking, the mathematical modeling of rubber is very difficult. The modeling of tires is even more difficult due to the irregular shape of a tire track surface and the very wide scope of load conditions. Also, tire characteristics change with the aging of tire materials. There are a few empirical tire models more widely used than mathematical models [19]. Empirical tire models express tire forces as a function of tire longitudinal and lateral slips, tire normal force, and surface conditions. The tire longitudinal slip is defined by the difference between a true absolute vehicle speed, equivalent to a free rotating wheel speed, and an actual measured wheel speed after being normalized by the same vehicle speed. Unfortunately, the absolute vehicle speed cannot be measured easily. The normal force has direct effect on wheel dynamics, but cannot be measured at a low cost. Also, it is rather safe to say that the surface condition is unknown in real time. Fig. 1 shows typical longitudinal friction (μ) curves as a function of a wheel slip on several surface conditions for cases without a wheel side slip.

The longitudinal slip of wheel is defined as

$$\lambda = \frac{\mathrm{V_{car}} - \mathrm{V_w}}{\mathrm{V_{car}}}. \tag{1}$$

As the figure shows, there is a wide variation of peak slip points and peak friction (μ) values depending upon surface types. For example, wet Jennite and gravel surfaces have similar peak μ values, but the peak slip points are far apart. Combining this wide variation with the even wider variation of tire normal load especially on deformable surfaces like gravel and unpacked snow, it is safe to say that any ABS algorithm that depends heavily on an accurate tire model would not work well in nonideal real-world situations.

III. Conventional ABS

In this section, the control algorithm of a typical conventional ABS is reviewed, and the limitation of its functionality is discussed. As mentioned in Section I, the algorithm is comprised of apply, hold, and dump modes.

Fig. 2 shows the typical data trace of a conventional ABS on a homogeneous high-μ surface. While the wheel speed is recovering from a large departure (a–b), the wheel pressure is held constant. When the wheel speed is judged to be fully recovered (b), the wheel pressure is applied (b–c) according to a predetermined schedule in open loop control. If any unscheduled event happens before the apply schedule is completed, the apply mode can be terminated. Otherwise, the pressure apply is held briefly (c–d). If any large departure of the wheel speed is not observed during the brief pressure hold mode, the pressure is finally reapplied (d–e) to induce the departure of the wheel speed. Finally, the pressure is dumped until the wheel speed departure is reduced and/or the wheel acceleration reaches a certain acceleration threshold (e–f). Then, a next cycle pressure hold mode starts (f–g).

Tuning the rule-based control algorithm is a very time consuming process. Even if the algorithm is tuned perfectly, it suffers some inherent flaws. The cycling of wheel speeds is inevitable to find the optimal slip (peak slip) that induces peak friction. However, the excessive cycling of wheel speed around the peak slip reduces average friction and also increases the fluctuation of friction. The effects are much worse for the front-wheel cycling of high center-of-gravity vehicles like sport utility vehicles (SUV) on a high-μ surface, since as much as 90% of total vehicle weight can be shifted to front wheels during heavy braking. It is also very critical to detect the transition of the surface (μ) quickly. Slow detection of a transition to high μ leads to the longer stopping distance due to underbraking. Also, slow detection to low μ leads to vehicle instability due to the excessive amount of wheel slip for an elongated time period. Unfortunately, the transition of μ during the fully recovered period of wheel cycling modes (a–b, or f–g) is very difficult to detect.

Another issue of the conventional ABS is turning stability. ABS can be activated during severe turning maneuvers. Wheel lateral friction is affected by wheel longitudinal slips. Therefore, the cycling front-wheel slips can cause significant noise, vibration, and harshness (NVH) and vehicle instability especially during braking and turning combined maneuvers. Other known issues of the rule-based control algorithm include but are not limited to the lack of robustness to different tires, uphill/downhill braking, vehicle loading condition and driver pedal pumping.

IV. Advanced ABS With Continuous Slip Control

In this section, a new continuous slip control ABS algorithm is developed with an intention to be implemented on existing production ABS harness without any modification or addition of sensor(s). During a normal driving condition without ABS activation, apply valves stay open and dump valves stay closed. If ABS is activated, the both valves are closed and wheel brake pressure is isolated from master cylinder pressure. When more wheel pressure is commanded by ABS, apply valves open. However, actual fluid flow—and therefore the amount of pressure increment—is determined by the pressure head across the valve. In reality, the apply valve can open just to speed up draining the fluid to master cylinder. This can happen due to the pumping of a brake pedal by a driver. It is very hard for the conventional rule-based controller to distinguish the difference between pedal pumping and a surface transition. On the other hand, the pressure head across a dump valve is always the same as wheel pressure which can be assumed to be proportional to vehicle deceleration. Therefore, the pressure drop during a dump mode can be estimated fairly accurately through the known dump command. By monitoring the wheel recovery and the pressure drop during a dump mode, surface conditions like the slop of a μ-slip curve can be estimated. Out of the estimated slop of a μ-slip curve, approximate optimal peak slip and therefore a desired wheel speed can be calculated.

In this advanced ABS algorithm, a vehicle is imagined as two bicycles. On each bicycle, a rear wheel and a front wheel are assumed to follow the same surface and trajectory. This assumption is reasonable above a certain vehicle velocity since the front and the rear wheels are on the same friction surface except for a short moment of surface transition. For example, for a vehicle with 2.5 m of wheel span and 100 km/h of longitudinal speed, the travel time delay between the wheels to pass the same spot is less than 0.1 s. At a lower speed, the time delay is increased. However, in terms of vehicle stopping distance, the braking performance of ABS at a low speed is not as important as that at a high speed. Also, the front-wheel speed control algorithm is designed to find a true optimal slip point around the target speed calculated out of rear-wheel speed information.

Rear wheels are allowed to cycle independently by continuous feedback control instead of the rule-based control. While cycling rear wheels, the optimal amounts of wheel slips are calculated. From the calculated optimal slips of rear wheels, desired front-wheel speeds are calculated. With front-wheel continuous slip control, front wheels are controlled to stay at optimal slip points. The main concept of continuous control algorithm is described in the following subsections.

The actual application of this concept on a real vehicle is a lot more complex with many minor details added to work for a very wide spectrum of real-world driving conditions. The conditions to be considered include but are not limited to deformable surfaces, surface transition, checker board, split friction, bumps/potholes, turning and braking, uphill/downhill, and mismatch tires. The developed control concept can be applied equally well to FWD and RWD systems with no difference to the control algorithm except for a few minor details. 4WD can make a difference if it has a hard-coupled-type center differential. Since this type of differential box is disappearing from the market especially for the vehicles equipped with ABS, hard-coupled 4WD is not considered in this study. There have been many efforts to estimate vehicle speed during ABS activation. None of the estimations are accurate but fairly good enough for the application on ABS. Therefore, the algorithm to estimate vehicle velocity is excluded from the scope of this study.

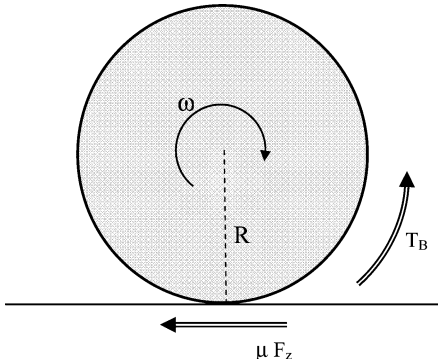

Fig. 3. Diagram of a rear-wheel control system.

A. Rear Wheel Cycling Control

Usually, feedback control algorithms are designed to stabilize a controlled system and also to minimize a tracking error. The lag on a feedback term always makes the tracking performance deteriorated. In this case, the good tracking control of rear-wheel speed is not meaningful since desired rear-wheel target speed is not well defined. As mentioned briefly at the beginning of Section IV, the optimal slip or the optimal wheel velocity can be estimated by monitoring cycling wheel speed and dump valve command. For a flat surface with a given wheel pressure, the change rate of wheel deceleration exceeds a certain threshold if the wheel slip is over a peak slip point. Since vehicle acceleration and jerk are limited physically, the desired rear-wheel velocity (ω_{Rdes}) is estimated simply by limiting measured wheel speed within a certain physical boundary and smoothing it by a low-pass filter [20]. However, this estimation gives just the approximate range of the optimal value since the estimation process is corrupted by wheel speed noise, wheel load change, surface change, and other uncertainties. Therefore, it is necessary to make the rear wheels find the optimal slip velocity using the desired rear-wheel velocity.

In this section, a new control strategy is developed for the wheel speed to cycle around an approximately optimal rear-wheel speed such that the range of the cycling wheel speed includes a true optimal slip speed. The rear wheels are rather forced to become unstable and to cycle around a peak slip point which is not well known by introducing lag in feedback control command intentionally. The controller is defined to be simple PD type.

The diagram of a rear-wheel control system is shown in Fig. 3. The wheel dynamics can be expressed as follows:

$$\mathrm{I_w}\dot{\omega} = \mu \mathrm{R F_z} - \mathrm{T_B}. \tag{2}$$

It needs to be reminded that, the change rate of brake pressure (or brake torque) is proportional to fluid flow rate, and flow rate is proportional to control valve opening. Therefore, the brake pressure rate is proportional to the valve command. Since the

brake control command is PD-type with an intentionally introduced first-order phase lag, the change rate of brake torque can be expressed as follows:

$$\dot{\mathrm{T}}_{\mathrm{B}} = \mathrm{u}_{\mathrm{R1}} \tag{3}$$

$$\dot{\mathrm{u}}_{\mathrm{R1}} = -\mathrm{a_c}\lfloor \mathrm{u_{R1}} - \mathrm{k_p}(\omega - \omega_{\mathrm{Rdes}}) - \mathrm{k_d}(\dot{\omega} - \dot{\omega}_{\mathrm{Rdes}})\rfloor. \tag{4}$$

It should be noted that the relationship between the brake pressure and the total flow volume is not linear but still monotonic. Therefore, the partial derivative of the pressure with respect to the flow is always positive. Combining (3) and (4)

$$\ddot{\mathrm{T}}_{\mathrm{B}} + \mathrm{a_c}\dot{\mathrm{T}}_{\mathrm{B}} = \mathrm{a_c k_p}(\omega - \omega_{\mathrm{Rdes}}) + \mathrm{a_c k_d}(\dot{\omega} - \dot{\omega}_{\mathrm{Rdes}}). \tag{5}$$

Combining (2) and (5), a closed-loop dynamic equation can be described as follows:

$$\mathrm{I_w}\ \dddot{\omega} + \mathrm{a_c I_w}\ddot{\omega} + \mathrm{a_c k_d}\dot{\omega} + \mathrm{a_c k_p}\omega = (\mu\ddot{\mathrm{R}}\mathrm{F_z}) + \mathrm{a_c}\,(\mu\dot{\mathrm{R}}\mathrm{F_z}) + \mathrm{a_c k_d}\dot{\omega}_{\mathrm{Rdes}} + \mathrm{a_c k_p}\omega_{\mathrm{Rdes}}. \tag{6}$$

It is generally assumed that tire normal load Fz is unchanged during a short time period or changed very slowly compared to the fast wheel dynamics. Also, the friction μ is constant around the peak slip point. Since vehicle speed is changing very slowly compared to wheel speed and the desired rear-wheel speed is proportional to the vehicle speed, it is further assumed that the time derivative of ω_{Rdes} is negligible. Therefore, (6) can be simplified as follows:

$$\mathrm{I_w}\ \dddot{\omega} + \mathrm{a_c I_w}\ddot{\omega} + \mathrm{a_c k_d}\dot{\omega} + \mathrm{a_c k_p}\omega = \mathrm{a_c k_p}\omega_{\mathrm{Rdes}}. \tag{7}$$

The characteristic equation of the closed-loop system given in (7) can be written as follows:

$$\mathrm{I_w S^3} + \mathrm{a_c I_w S^2} + \mathrm{a_c k_d S} + \mathrm{a_c k_p} = 0. \tag{8}$$

By Routh's stability criterion [21], the system is unstable for

$$\mathrm{a_c} < \frac{\mathrm{k_p}}{\mathrm{k_d}}. \tag{9}$$

Therefore, for a small enough $\mathrm{a_c}$ (a large phase lag), the closed-loop system becomes unstable. In reality, μ is not a constant and rather a linear function of a slip (λ) for the linear region where the slip is small, i.e.,

$$\mu = \mu_0\lambda = \mu_0\frac{\mathrm{V_{car}} - \mathrm{R}\omega}{\mathrm{V_{car}}}. \tag{10}$$

Combining (10) with (2)–(4), the closed-loop system characteristic equation can be written as follows:

$$\mathrm{I_w S^3} + (\mathrm{a_c I_w} + \mu_0\mathrm{R^2F_z/V_{car}})\mathrm{S^2} + \mathrm{a_c}\,(\mu_0\mathrm{R^2F_z/V_{car}} + \mathrm{k_d})\mathrm{S} + \mathrm{a_c k_p} = 0. \tag{11}$$

Similar Routh's stability analysis shows that the system is stable for

$$\mathrm{a_c} > \mathrm{MAX}\left[\left(\frac{\mathrm{k_p}}{\mu_0\mathrm{R^2F_z/V_{car}} + \mathrm{k_d}} - \frac{\mu_0\mathrm{R^2F_z/V_{car}}}{\mathrm{I_w}}\right), 0\right]. \tag{12}$$

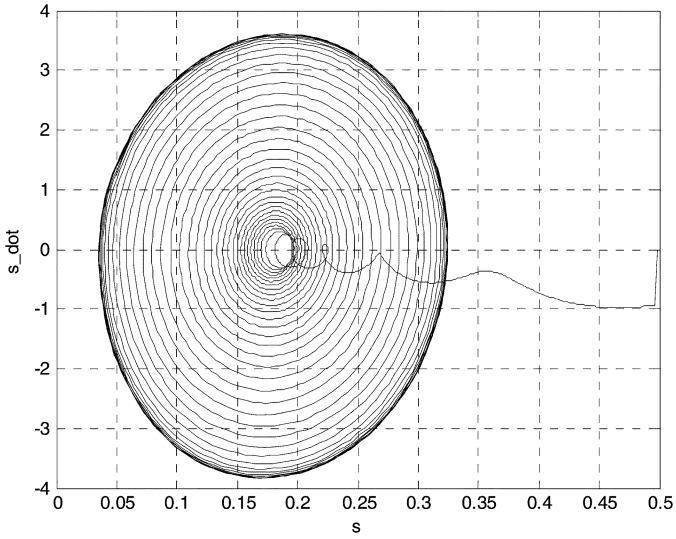

Fig. 4. Stable limit cycle in a phase plane.

Therefore, in the linear region of a μ-slip curve where μ_0 is a large positive constant, the closed-loop system is stable even for a very small $\mathrm{a_c}$, i.e., for a large control phase lag, or always stable for the proper combination of the feedback gains $(\mathrm{k_p}, \mathrm{k_d})$. Therefore, the rear wheels create stable limit cycles for the appropriate amount of the phase lag and the target wheel speed defined around or over the peak slip point. Fig. 4 shows an example of a stable limit cycle created in simulation with the model of a typical dry surface μ-slip curve and the feedback controller with the phase lag described in (3) and (4).

The optimal amount of phase lag, that induces an appropriate amount of cycling depth, can be defined as a function of estimated and measured vehicle states. However, it needs to be fine tuned by the vehicle testing on a real test track considering the irregular shape of real μ-slip curves, surface irregularity, a brake actuation lag, wheel speed sensor noise, and other uncertainties. Also, the brake control gains need to be tuned as the function of surface irregularity. For example, on an irregular surface, wheel speed tends to become very jerky. This can be interpreted as accelerating wheel departure that leads to the overdumping command of brake pressure. The surface irregularity can be estimated by monitoring the moving average of wheel jerk.

B. Front-Wheel Slip Control

By monitoring the cycling pattern of rear wheels, the optimal wheel speed inducing peak μ is calculated on each side of a vehicle. The optimal wheel speed is represented by the point where wheel deceleration increases rapidly compared to slowly changing wheel pressure. Considering the fact that the optimal speed is not accurate, and an insufficient wheel slip can cause significant underbraking, some amount of extra slip margin is added to define desired front-wheel speed (ω_{Fdes}) as follows:

$$\lambda = (1 + \mathrm{g_f})\lambda_{\mathrm{Rdes}} \quad , \mathrm{g_f} > 0 \tag{13}$$

where λ and λ_{Rdes} are the desired slips of front and rear wheels equivalent to ω_{Fdes} and ω_{Rdes}. By adding some slip margin

to the optimal speed, front-wheel target speeds—one on each side—are defined to be on or over the optimal slip points. Since the front wheels are intended to follow the target speeds tightly without cycling, a simple PD-type controller is tried but with no additional phase lag. The stability of the closed-loop control system is analyzed under the assumption that a μ-slip curve is locally linear, i.e.,

$$\dot{\mu} = \mathrm{k}_0 \dot{\lambda} \tag{14}$$

where k_0 can be positive, zero or negative depending on the region of the μ-slip curve. Since vehicle speed changes much slowly compared to wheel speed, (1) and (14) can be combined with the time derivative of vehicle speed neglected as follows:

$$\dot{\mu} = -\mathrm{k}_0 \frac{\mathrm{R}}{\mathrm{V_{car}}} \dot{\omega}. \tag{15}$$

It can be assumed similarly to the front wheels that the normal load Fz changes slowly. Therefore, the differentiation of (2) is described as follows:

$$\mathrm{I_w} \ddot{\omega} = \dot{\mu} \mathrm{R} \mathrm{F_z} - \dot{T}_\mathrm{B}. \tag{16}$$

If a simple PD-type controller is chosen similarly to the rear-wheel controller but without an intentional phase lag, control input can be described as follows:

$$\dot{T}_\mathrm{B} = -\mathrm{k_p}(\omega - \omega_\mathrm{Fdes}) - \mathrm{k_d}(\dot{\omega} - \dot{\omega}_\mathrm{Fdes}). \tag{17}$$

Combining (15), (16), and (17), a closed-loop dynamic equation is derived as follows:

$$\mathrm{I_w} \ddot{\omega} + \left(\mathrm{k_d} + \mathrm{k}_0 \frac{\mathrm{R}^2 \mathrm{F_z}}{\mathrm{V_{car}}} \right) \dot{\omega} + \mathrm{k_p} \omega = \mathrm{k_p} \omega_\mathrm{des} + \mathrm{k_d} \dot{\omega}_\mathrm{des}. \tag{18}$$

The characteristic equation of the closed-loop control system described in (18) is expressed as follows:

$$\mathrm{I_w S}^2 + \left(\mathrm{k_d} + \mathrm{k}_0 \frac{\mathrm{R}^2 \mathrm{F_z}}{\mathrm{V_{car}}} \right) \mathrm{S} + \mathrm{k_p} = 0. \tag{19}$$

As (19) shows, the closed-loop system is always stable for the stable region of the μ-slip curve where k_0 is positive. Also, the derivative gain $\mathrm{k_d}$ can be chosen to be large enough to make the system stable around and just past the peak slip where k_0 is zero or slightly negative. The magnitude of the derivative gain is limited by the noise level of wheel speed signals though. Also, the performance of the closed-loop control is affected by actuation performance limit.

The above PD-type front-wheel control scheme is working fine for most surfaces except for a wet Jennite surface shown in Fig. 1 and other very peaky surfaces. If the slip passes the peak point, the friction coefficient of the wet Jennite surface drops significantly. Therefore, even a slight amount of excessive target slip can cost stopping distance significantly. Also, it is practically impossible to define the exact target wheel speed that represents the peak slip. To deal with this kind of unusual and extreme surface condition, the PD-type controller described in (17) is modified with an additional double derivative error feedback term which is applied asymmetrically only when the control error rate is negative, i.e.,

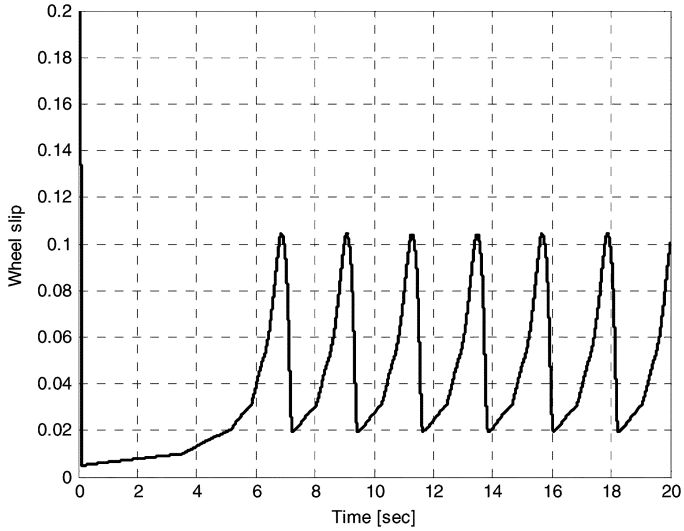

Fig. 5. Front-wheel control with a PD-type controller.

$$\begin{aligned} &\mathrm{IF}, \dot{\omega} - \dot{\omega}_\mathrm{Fdes} > 0 \\ &\dot{T}_\mathrm{B} = -\mathrm{k_p}(\omega - \omega_\mathrm{Fdes}) - \mathrm{k_d}(\dot{\omega} - \dot{\omega}_\mathrm{Fdes}) \\ &\mathrm{ELSE} \\ &\dot{T}_\mathrm{B} = -\mathrm{k_p}(\omega - \omega_\mathrm{Fdes}) - \mathrm{k_d}(\dot{\omega} - \dot{\omega}_\mathrm{Fdes}) - \mathrm{k_{dd}}(\ddot{\omega} - \ddot{\omega}_\mathrm{Fdes}). \end{aligned} \tag{20}$$

The controller suggested in (20) is validated by simulation on a very peaky surface similar to the wet Jennite surface described in Fig. 1. Initially, friction increases very stiffly proportional to a slip. When the slip passes a peak point ($\mathrm{s} = 0.02$), friction decreases equally rapidly before it becomes stabilized and decreases gradually.

For the simulation, a target slip is set to be 0.05. Targeting slip error is only 0.03, but the resulting loss of surface friction is as much as 10% from the peak value. Fig. 5 shows the simulation result of the original tracking controller defined in (17). Due to the severe negative slop of the friction-slip curve at the target slip point (0.05), the control becomes unstable. It is possible to track the target slip by increasing the differential gain—shown in Fig. 6. This is possible only if a brake actuator is fast enough. However, the good tracking control of the suboptimal target slip is not the goal of good ABS algorithm design. Fig. 7 shows the simulation result of the front-wheel control with the modified controller described in (20). There exists steady state tracking error, but the wheel slip rather follows the optimal slip point (0.02) automatically. Therefore, the goal of the front-wheel slip control with maximized friction is achieved.

V. Test Results

The performance of developed advanced continuous slip ABS is implemented on several test vehicles using d-Space, and evaluated on diverse surface conditions. The true vehicle speed and the wheel pressures are measured only for the purpose of monitoring and are unknown to ABS algorithm.

Fig. 8 shows the performance of advanced ABS implemented on a BMW 740i and tested on a dry asphalt surface.

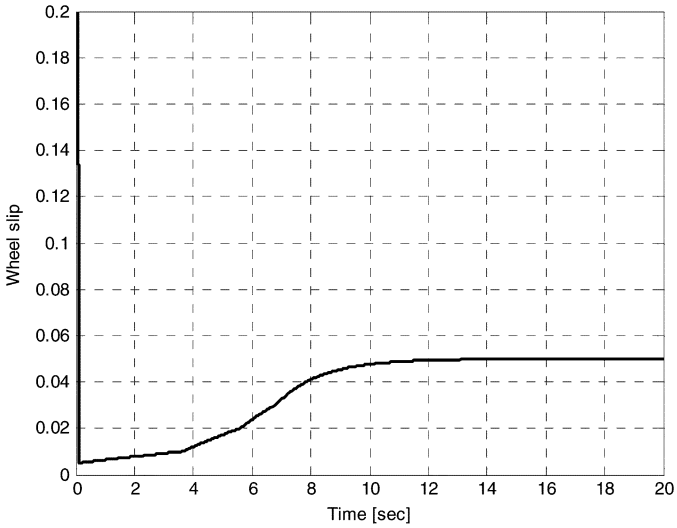

Fig. 6. Front-wheel control with a PD-type controller—increased differential control gain.

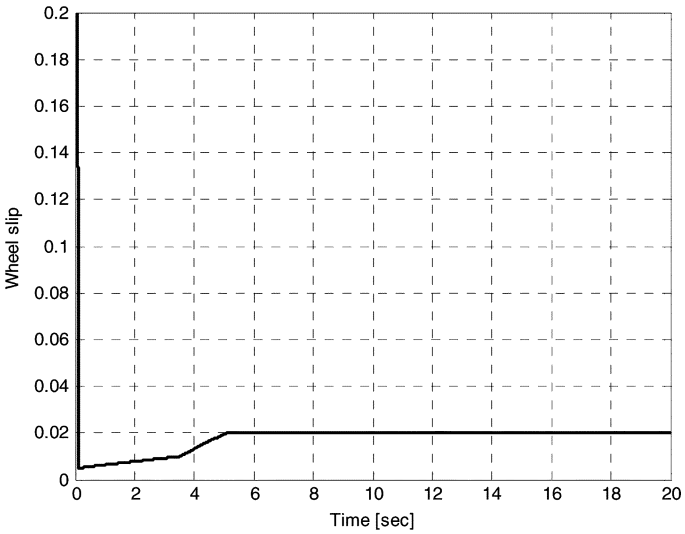

Fig. 7. Front-wheel control with a PD+DD-type controller.

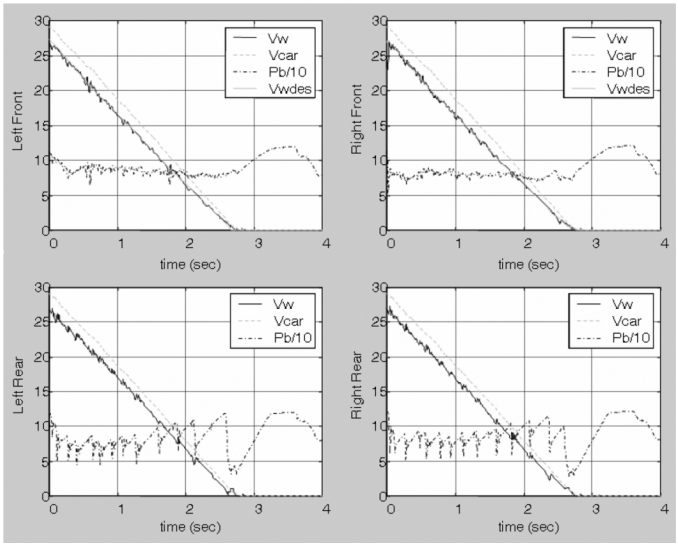

Fig. 8. Advanced ABS on dry asphalt.

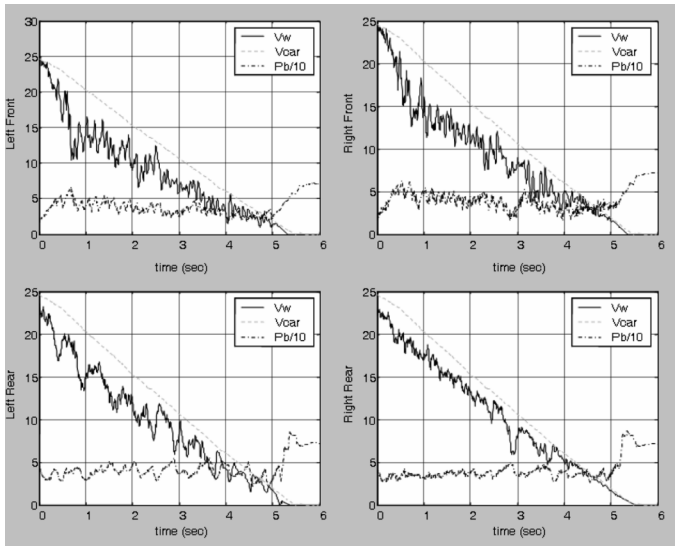

Fig. 9. Advanced ABS on loose gravel.

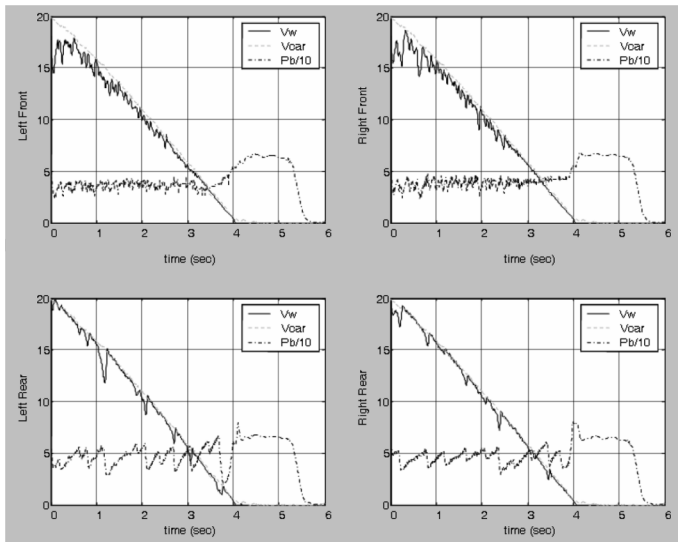

Fig. 10. Advanced ABS on wet Jennite.

Rear wheels are tuned to cycle faster than the cycling frequency of conventional ABS. In this way, rear wheels consume a little bit more fluid but find optimal slips much faster. Front wheels follow optimal target wheel speeds without cycling. Since front brake channels have much more fluid capacity than rear ones for the same pressure level, noncycling front wheels save a significant amount of fluid consumption. Vehicle deceleration exceeds 1.0 g and approaches very close to the physical friction limit of the surface.

Fig. 9 shows the performance of advanced ABS implemented on a Ford Windstar minivan and tested on a loose gravel surface. As Fig. 1 shows, this kind surface needs a deep slip to achieve optimal friction. Front wheels follow an optimal slip fairly well in the sense of average considering a loose and bumpy surface condition. Also, front wheels hold fairly constant brake pressure.

Fig. 10 shows the performance of advanced ABS implemented on the same minivan and tested on a wet Jennit surface. Jennite has a very peaky characteristic μ-slip curve. As Fig. 1

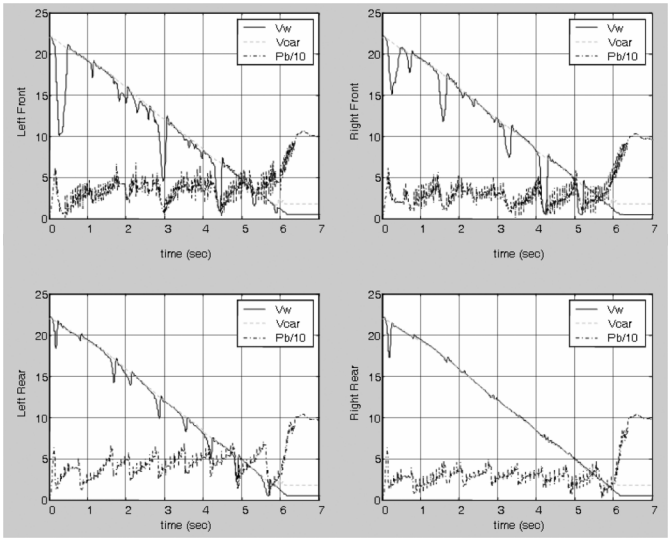

Fig. 11. Conventional ABS on wet Jennite.

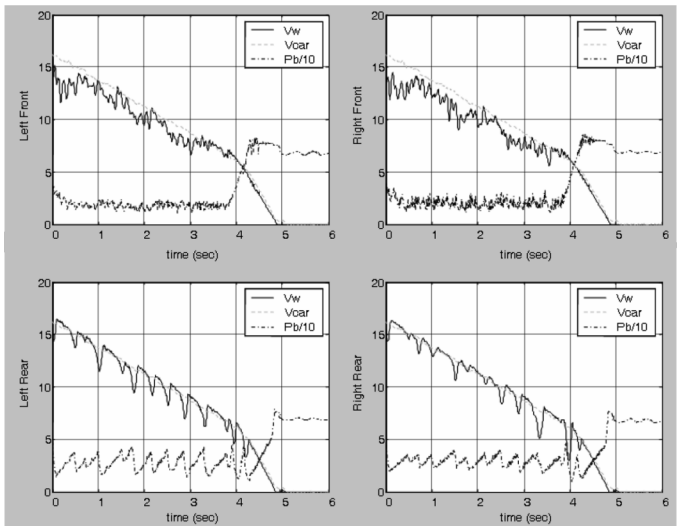

Fig. 12. Advanced ABS on a surface transition condition.

shows, peak μ is at less than 3% slip. For any slight offset from the peak slip, $\mu$is reduced significantly. Therefore, it is one of the most difficult surfaces to achieve a good control performance. Front-wheel slip and pressure show that the control is very robust. Front wheels show no sign of underbraking or overslip. The control performance is quite distinguished compared to that of a conventional production ABS tested using the same vehicle on the same surface that is shown in Fig. 11. Average vehicle deceleration is much lower, and the variation of wheel pressure is much larger—the worst combination. The departures of front-wheel speeds are quite significant.

Fig. 12 shows the performance of advanced ABS implemented on the same minivan. The quick response to surface transition even without any transition detection algorithm is the virtue of the developed ABS algorithm. The surface transition from wet tile to concrete happens at 3.8 s. At the moment of the surface transition, front-wheel slips are reduced significantly, and the constant slip controller increases wheel pressure immediately. The rise rate of brake pressure is limited only by the

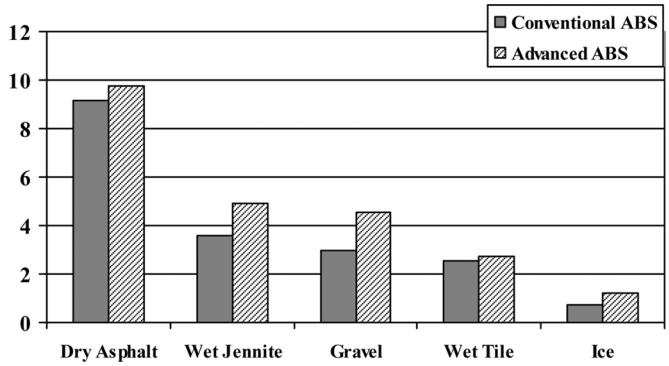

Fig. 13. Average deceleration [m/second^2].

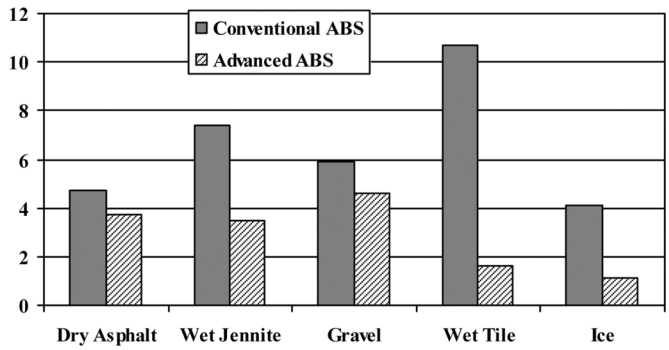

Fig. 14. Average flow rate normalized by deceleration [cc/second]/[m/second^2].

brake actuation performance, i.e., the pumping capability of ABS pump/motor and the size of the hydraulic valves.

VI. Comparison of Advanced ABS With Conventional ABS

In this section, the performance of advanced continuous slip ABS is compared with that of conventional ABS. The best ABS maximizes vehicle deceleration while minimizing NVH. NVH is mostly associated with the fluctuation of brake pressure and brake pedal feedback. Since both of them are well represented by the fluctuation of brake fluid flow, the average flow rate, and the flow rate variance of the brake fluid are compared along with vehicle deceleration. Both ABS algorithms are tested on a Ford Windstar minivan, and the performances are compared on several homogeneous μ surfaces.

Fig. 13 compares average vehicle decelerations. As the figure shows, the average deceleration is improved from about 5% on dry asphalt to as much as 40% on ice and other medium μ surfaces. With 5% improvement of stopping distance on dry asphalt, the braking performance reaches the physical limit of tire-to-surface friction. On a low μ surface like ice, it takes a long time for a deep departed wheel slip to recover to an optimal slip point. Therefore, the deep cycling wheel slip control of conventional ABS deteriorates braking performance significantly. Also, a deep cycling wheel slip causes the already low lateral friction to be reduced even further, and therefore the yaw dynamics stabilizing effect of ABS function is not fully utilized.

Fig. 14 compares average brake fluid consumption rates after being normalized by average vehicle decelerations during ABS

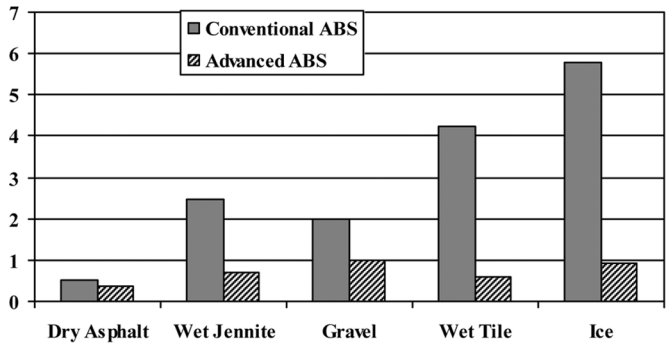

Fig. 15. Flow rate variance normalized by deceleration [cc/second]/[m/second^2].

activation. As the figure shows, conventional ABS requires significantly more brake fluid flow for the same level of vehicle deceleration, and this large flow rate is due to the deep cycling control of front wheels. The fluid overconsumption of conventional ABS is observed through the wide range of surface conditions. Due to the large flow rate, conventional ABS requires a larger pump or the same sized pump forced to be operated at a higher speed. The high-speed operation of the pump causes a significant amount of noise, and this pump noise is dominant especially on low μ surfaces where the pump noise is not masked enough by other noise induced by a tire slip.

Fig. 15 compares the variances of brake flow rate after being normalized by average vehicle decelerations during ABS activation. It is very critical to minimize the flow variance since it has the most adverse effect on pedal feeling and other NVH. It should also be noted that ABS pump/motor is sized to handle the worst case flow rate, and the pump/motor has to be sized up as the flow variance is increased. The figure shows the significant improvement of flow characteristics through the whole range of surface conditions. The normalized variance of fluid flow is reduced at least 25% on dry asphalt and as much as 85% on ice. Also, the figure shows that the surface-to-surface variation of variance is also minimized. Therefore, advanced ABS shows very good NVH characteristics that are consistent with the expectations of drivers, e.g., quiet for a smooth low μ smooth surface and a little bit harsher for a bumpy deformable surface.

VII. Conclusion

An ABS algorithm with a continuous wheel slip control has been developed and implemented on existing production ABS harness with no extra sensors and no modification of brake actuators. Front-wheel pressures are controlled to stay almost constant, and front-wheel speeds track optimal friction speeds fairly well. With a simple continuous feedback control, rear wheels are realized to cycle around peak slip points. The depth of the cycling wheel slip is shown to be well tunable. Total tuning parameters are reduced from hundreds for conventional ABS down to a dozen for advanced ABS. Therefore, the tuning time is reduced from almost two years to just one week. It is a big impact especially for the applications on small volume products. With reduced tuning parameters and a simple analytical control algorithm, ECU memory space is also saved significantly.

Due to the optimal continuous slip control of front wheels, stopping distance is reduced up to 40% depending on the control surfaces. On dry asphalt, 1.1 g vehicle deceleration is achieved. This number approaches the physical limit of the surface friction very closely. With the reduction of brake fluid flow and also flow fluctuation, brake pedal feedback and other vehicle NVH characteristics are improved significantly. Also, more stable steering response is achieved during braking and turning combined maneuvers.

References

[1] H. Leiber and A. Czincze, Antiskid system for passenger cars with a digital electronic control unit. Soc. Automobile Eng., Washington, DC, SAE 790458, 1979.
[2] D. Pavkovic, J. Deur, J. Asgari, and D. Hrovat, Experimental analysis of potentials for tire friction estimation in low-slip mode. Soc. Automobile Eng., Washington, DC, SAE 2006-01-0556, 2006.
[3] M. Valardocchia and A. Sorniotti, Hardware-in-the-loop to evaluate active braking systems performance. Soc. Automobile Eng., Washington, DC, SAE 2005-01-1580, 2005.
[4] M. Salehi and G. Vossoughi, "Vehicle integrated control [ABS, ASUS, 4WS with variable structure control (sliding mode)]: The new method for active suspension system," in *ASME DETC*, Long Beach, CA, 2005.
[5] Y. Hou and Y. Sun, Fuzzy slide mode control method for ABS. Soc. Automobile Eng., Washington, DC, SAE 2004-01-0252, 2004.
[6] W. Ribbens and R. Fredricks, A sliding mode observer-based ABS for aircraft and land vehicles Soc. Automobile Eng., Washington, DC, SAE 2003-01-0252, 2003.
[7] J. Sun, Development of fuzzy logic anti-lock braking system for light bus. Soc. Automobile Eng., Washington, DC, SAE 2003-01-0458, 2003.
[8] V. Ivanov, M. Vysotsky, V. Boutylin, and J. Lepeshko, The theoretical concepts for pre-extreme ABS. Soc. Automobile Eng., Washington, DC, SAE 2002-01-2185, 2002.
[9] L. Jun, J. Zhang, and F. Yu, An investigation into fuzzy control for anti-lock braking system based on road autonomous identification. Soc. Automobile Eng., Washington, DC, SAE 2001-01-0599, 2001.
[10] S. Yamazaki, O. Furukawa, and T. Suzuki, "Study on real time estimation of tire to road friction," in *Vehicle System Dynamics Supplement 27*. Washington, DC: SAE, 1997.
[11] S. Drakunov, U. Ozguner, P. Dix, and B. Ashrafi, "ABS control using optimum search via sliding modes," *IEEE Trans. Control Syst. Technol.*, vol. 3, no. 1, Mar. 1995.
[12] Y. Chin, C. Lin, and M. Sidlosky, "Sliding mode ABS wheel slip control," in *Proc. Amer. Control Conf.*, 1992.
[13] A. Semsey, R. Roberts, and L. Ho, Simulation in the development of the electronic wedge brake. Soc. Automobile Eng., Washington, DC, SAE 2006-01-0298, 2006.
[14] S. Anwar, "Anti-lock braking control of an electromagnetic brake-by-wire system," in *ASME Int. Mech. Eng. Congr. Expo.*, Orlando, FL, 2005.
[15] O. Emereole and M. Good, "Comparison of the braking performance of electromechanical and hydraulic ABS systems," in *ASME Int. Mechanical Eng. Congr. Expo.*, Orlando, FL, 2005.
[16] R. Stence, Digital by-wire replaces mechanical systems in cars. Soc. Automobile Eng., Washington, DC, SAE 2004-01-2926, 2004.
[17] S. Raman, B. Shylandra, and M. Mahalingam, Beyond ABS-brake by wire development of a working concept. Soc. Automobile Eng., Washington, DC, SAE 2003-28-0010, 2003.
[18] P. Khatun, C. Bingham, and P. Mellor, Comparison of control methods for electric vehicle antilock braking/traction control systems. Soc. Automobile Eng., Washington, DC, SAE 2001-01-0596, 2001.
[19] E. Bakker, H. B. Pacejka, and L. Lidner, A new tire model with an application in vehicle dynamics studies. Soc. Automobile Eng., Washington, DC, SAE 890087, 1989.
[20] S. Choi and D. Milot, "An anti-lock brake system with continuous wheel slip control," U.S. Patent Appl. 04715675.7-2423-US2004005970, 2004.
[21] Ogata, *Modern Control Engineering*. Englewood Cliffs, NJ: Prentice-Hall, 1970.